Proceedings of the 2003 IEEE/RSJ
Intl. Conference on Intelligent Robots and Systems
Las Vegas, Nevada · October 2003

# Kinematic Analysis and Design of a 6 DOF Haptic Master for Teleoperation of a Mobile Manipulator

†,††Dongseok Ryu, †,††Changhyun Cho, †Munsang Kim, ††Jae-Bok Song

† Advanced Robotics Research Center
Korea Institute of Science and Technology
39-1 Hawolgok-dong, Sungbuk-ku, Seoul 136-791
Korea

†† Department of Mechanical Engineering
Korea University
Anam-dong, Sungbuk-gu, Seoul 136-701
Korea

Abstract – In this paper, a new design of a 6DOF haptic master is presented, and the architectural parameters are discussed in consideration of the kinematic characteristics. This device was intended to teleoperate a mobile manipulator, which requires planar 3 DOF motion for navigation of the vehicle and full 6 DOF motion for manipulation. The proposed haptic master is composed of two parallel mechanisms, and each mechanism offers 3DOF independently. The spatial mechanism, which extends the workspace into 3D, is attached on the planar mechanism for vehicle operation. Since low inertia is vital to back−drivability and transparency of the haptic device, all actuators are placed on the base and thus some forces for haptic feedback are transmitted by the tendon-driven mechanism. This paper presents the kinematic analysis of the haptic master with respect to the workspace and the performance indices related to the Jacobian. The actual system was constructed with the architectural parameters determined on the basis of the analysis.

## I. INTRODUCTION

Recently, a great deal of work has been done in multi DOF haptic devices based on parallel mechanisms [1,2,3]. Since these devices employ parallel mechanisms as a basic configuration, high stiffness and accuracy can be achieved with relative ease. Moreover, it is easy to install all actuators near the fixed base, thus greatly reducing the mass and moment of inertia of the moving parts, and leading to enhanced back-drivability and transparency [4,5].

Some haptic applications require motion and force reflection in the whole 3D workspace (i.e., 6 DOF motion). Even for these applications, however, the device seldom needs the whole 6 DOF motion at all times during operation. In most 6 DOF haptic devices, all 6 actuators are activated to create force feedback even when only simple motion is desired, since the Cartesian space and joint space are closely coupled in the device.

It is desirable, therefore, that a haptic device be designed so that only the necessary DOFs are active while other DOFs remain inactive depending upon the situation. This strategy has several advantages. First, the computational burden needed to solve kinematic and static equations are greatly reduced. Second, it is energy efficient because only the necessary actuators are activated.

Although the proposed haptic master can be used for a variety of tasks, the original design concept focused on the teleoperation of a mobile manipulator. It was observed that most haptic devices tend to divide 3D motion into 3 DOFs in position (i.e., x, y, z translation) and 3 DOFs in orientation (e.g., roll, pitch, yaw). A close look at the teleoperation of a mobile manipulator reveals that it requires planar 3 DOF motion for navigation of the vehicle and full 6 DOF motion for manipulation. Therefore, the proposed haptic master consists of two independently working mechanisms; one is a planar 3 DOF parallel manipulator and the other is a spatial 3 DOF parallel manipulator [6]. Fig. 1 shows a proposed haptic master.

Fig.1 Photo of the proposed haptic master

The remainder of this paper is organized as follows. In Section 2, design of a proposed haptic device is introduced briefly. Section 3 describes the kinematic constraints and Jacobain of the device. Section 4 discusses the kinematic characteristics (e.g., workspace, performance indices related to Jacobian.) with respect to architectural parameters. Section 5 concludes the results.

## II. DESIGN CONCEPT AND STRUCTURE

The proposed haptic master is composed of upper and lower mechanisms as shown in Fig. 1. Both mechanisms are constructed in the form of a parallel mechanism to ensure high stiffness and accuracy. The upper mechanism is attached serially to the end-effector of the lower mechanism to form a 6 DOF haptic master. In what follows, the upper and lower mechanisms are discussed in detail.

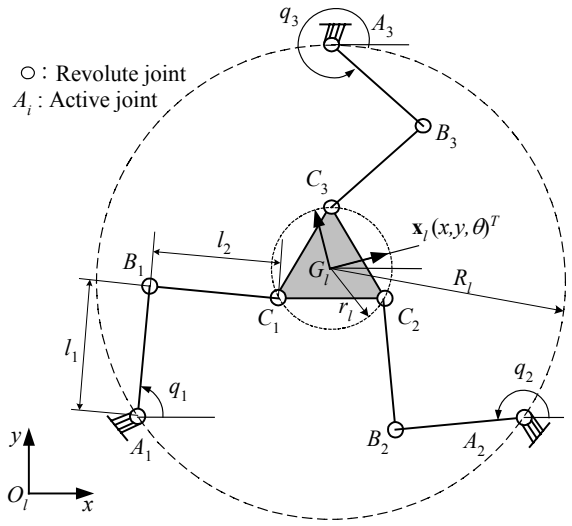


Fig. 2 Schematic of the lower mechanism.

The lower mechanism is designed to be a planar 3 DOF parallel manipulator. Since back-drivability of a prismatic joint is not as good as that of a revolute joint, a RRR limb structure, comprising 2 links and 3 revolute joints, is adopted in this design as shown in Fig. 2. Joints $A_i$ are active while the remaining joints are passive. It is seen that actuation of active joints enables the platform to perform 3 DOF motion of ($x$, $y$, $\theta$).

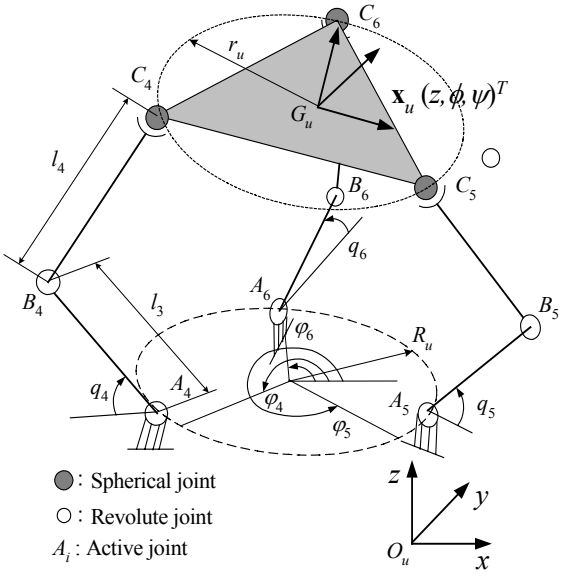


Fig. 3 Schematic of the upper mechanism.

The upper mechanism is designed as a spatial 3 DOF parallel manipulator. 3 RRS spatial parallel mechanisms are employed as shown in Fig.3. Actuation of active joints $A_i$ enables the triangular end-effector to perform 3 DOF motion of ($z$, $\phi$, $\psi$).

Finally, a new 6 DOF haptic master is constructed by putting both mechanisms together serially as shown in Fig.4. It is noted that both upper and lower mechanisms are independent of each other in 3D motions. For instance, if only planar motion is required, the 3 DOFs of the lower mechanism are sufficient to provide this motion. This is particularly important feature for force reflection.

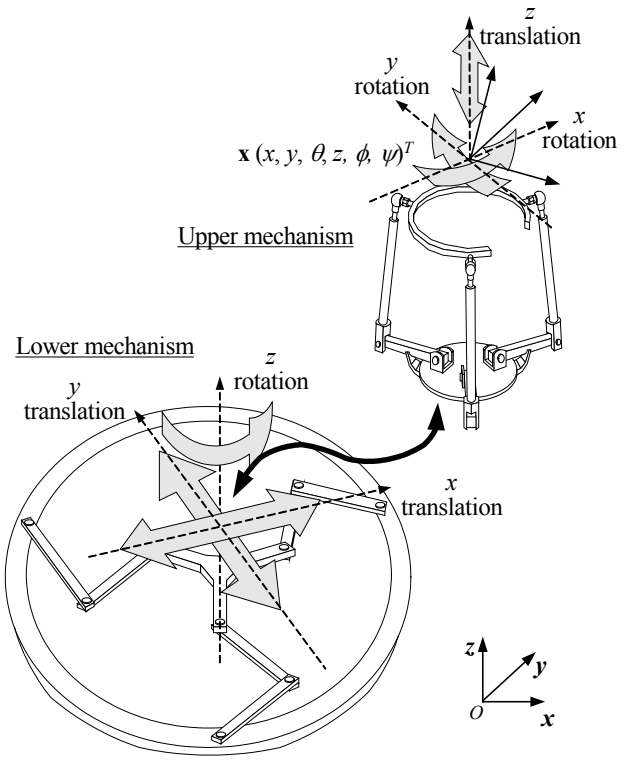


Fig. 4 Structure of the proposed haptic master.

In most 6 DOF haptic devices, all 6 actuators are activated to create force reflection even when only simple motion is involved, because the Cartesian space and joint space are closely coupled. In the proposed haptic device, however, the upper and lower mechanisms are decoupled to some extent, so force reflection problem becomes simpler to solve.

If the 3 actuators to drive the upper mechanism are placed on the end-effector of the lower mechanism, which corresponds to the base of the upper mechanism, they are forced to move with the lower mechanism. In this case a user must exert more force due to the added mass of the actuators, thus, back-drivability of the device is significantly reduced. One solution to this problem is to adopt a tendon-driven mechanism in which actuators can be placed on the base which is fixed during operation. As shown in Fig. 5, tendon pulleys for tendon are placed at the revolute joints of the limbs of the lower mechanism. Although the proposed tendon structure has the disadvantage of coupling the motion between the two mechanisms, the increase in back-drivability far outweighs the disadvantages.

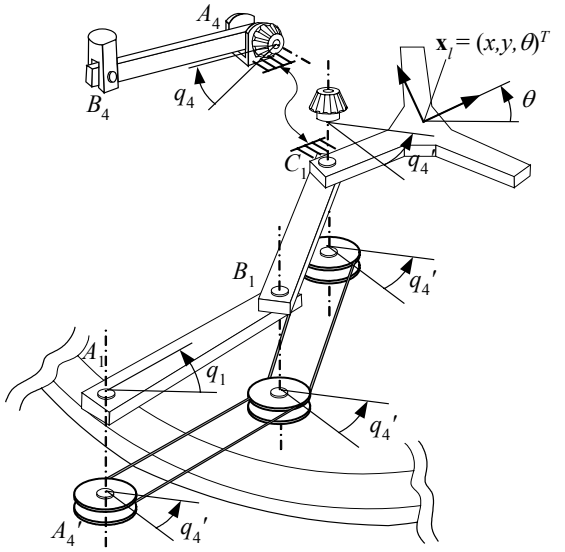


Fig. 5 Schematic of tendon-driven mechanism for force transmission.

## III. JACOBIAN ANALYSIS

In order to operate the haptic device, we need to find the kinematic equations which relate joint variables to Cartesian variables. Although the whole system is of 6 DOFs, the device can be decomposed into the upper and lower mechanisms, which makes derivation of kinematic equations easier.

Let the pose (i.e., position and orientation) of the end-effector be described by a vector **x** and the actuated joint variables by a vector **q** as follows:

$$\mathbf{x}_l = \{x \quad y \quad \theta\}^T,\ \mathbf{x}_u = \{z \quad \phi \quad \psi\}^T$$
$$\mathbf{x} = \begin{Bmatrix} \mathbf{x}_l \\ \mathbf{x}_u \end{Bmatrix} \tag{1}$$

$$\mathbf{q}_l = \{q_1 \quad q_2 \quad q_3\}^T,\ \mathbf{q}_u = \{q_4' \quad q_5' \quad q_6'\}^T$$
$$\mathbf{q} = \begin{Bmatrix} \mathbf{q}_l \\ \mathbf{q}_u \end{Bmatrix} \tag{2}$$

where the subscripts *l* and *u* denote the lower and upper mechanisms, respectively. Note that all the variables were shown in Fig. 2 and 3.

The kinematic relations are written in vector form. Eqn. (3) is for the lower mechanism, and Eqn. (4) is for upper one.

$$\overrightarrow{A_iG_l} + \overrightarrow{G_lC_i} = \overrightarrow{A_iB_i} + \overrightarrow{B_iC_i}, \quad i = 1,2,3 \tag{3}$$

$$\overrightarrow{A_iG_u} + \overrightarrow{G_lC_i} = \overrightarrow{A_iB_i} + \overrightarrow{B_iC_i}, \quad i = 4,5,6 \tag{4}$$

Constraints can be derived from the observation that the length of the distal link, $B_iC_i$, remains a constant length, $l_2$. It is written as follows.

$$\begin{aligned} &f_i(x, y, \theta, q_i) = \\ &[(x + x_{G_lC_i} \cdot c\theta - y_{G_lC_i} \cdot s\theta) - (x_{A_i} + l_1 c(q_i))]^2 \\ &+[(x + x_{G_lC_i} \cdot c\theta - y_{G_lC_i} \cdot s\theta) - (x_{A_i} + l_1 c(q_i))]^2 \\ &-{l_2}^2 = 0, \quad i = 1,2,3 \end{aligned} \tag{5}$$

$$\begin{aligned} &f_i(z, \phi, \psi, \theta, q_i) = \\ &\begin{pmatrix} x_{G_lC_i} \cdot c\theta \cdot c\phi + y_{G_lC_i}(-s\theta \cdot c\psi + c\theta \cdot s\phi \cdot s\psi) \\ -(l_3 c\varphi_i c(q_i) + x_{A_i}) \cdot \cos\theta + (l_3 s\varphi_i c(q_i) + x_{A_i}) \cdot s\theta \end{pmatrix}^2 \\ &+\begin{pmatrix} x_{G_lC_i} \cdot s\theta \cdot c\phi + y_{G_lC_i}(c\theta \cdot c\psi + s\theta \cdot s\phi \cdot s\psi) \\ -(l_3 c\varphi_i c(q_i) + x_{A_i}) \cdot s\theta - (l_3 s\varphi_i c(q_i) + x_{A_i}) \cdot c\theta \end{pmatrix}^2 \\ &+[z - x_{G_lC_i} \cdot s\phi + y_{G_lC_i} \cdot c\phi \cdot s\psi - l_3 s(q_i)]^2 - {l_4}^2 = 0, \\ &i = 4,5,6 \end{aligned} \tag{6}$$

All variables in the terms of Eqs. (5) and (6) were shown in Fig. 2 and 3, and the scripts, *s* and *c* are denoted the sine and cosine.

In the proposed haptic master, inevitably another constraint results from tendon driven mechanism described by

$$q_i = (q_i' + \theta), \quad i = 4,5,6 \tag{7}$$

where $q_i'$ is the angle created by the motor for the lower mechanism and $\theta$ is a function of $q_1$, $q_2$ and $q_3$. It follows that control of the upper mechanism requires control of the lower mechanism as well as control of $q_4'$, $q_5'$ and $q_6'$.

The differential relations between the joint and the Cartesian vectors for each mechanism can be derived from the constraint Eqs. (5) and (6) by

$$\mathbf{J}_{ql} \cdot d\mathbf{q}_l = \mathbf{J}_{xl} \cdot d\mathbf{x}_l \tag{8}$$

$$\mathbf{J}_{qu} \cdot d\mathbf{q}_u = \mathbf{J}_{xu} \cdot d\mathbf{x}_u \tag{9}$$

where $\mathbf{J}_{ql}$ and $\mathbf{J}_{xl}$ are the Jacobians of the lower mechanism, and $\mathbf{J}_{qu}$ and $\mathbf{J}_{xu}$ are the Jacobians of the upper mechanism, respectively. Using the definitions of Eqs. (1) and (2), Eqs. (8) and (9) can be integrated into a single equation

$$\mathbf{J}_q \cdot d\mathbf{q} = \mathbf{J}_x \cdot d\mathbf{x} \tag{10}$$

where

$$\mathbf{J}_q = \begin{bmatrix} \mathbf{J}_{ql} & \mathbf{0} \\ \mathbf{0} & \mathbf{J}_{qu} \end{bmatrix} = \mathrm{diag}[J_{q1}\, J_{q2}\, J_{q3}\, J_{q4}\, J_{q5}\, J_{q6}] \tag{11}$$

$$\mathbf{J}_x = \begin{bmatrix} \mathbf{J}_{xl} & \mathbf{J}_{xc1} \\ \mathbf{J}_{xc2} & \mathbf{J}_{xu} \end{bmatrix} \tag{12}$$

where $\mathbf{J}_q$ and $\mathbf{J}_x$ are the Jacobians of the haptic master, and $\mathbf{J}_{xc1}$ and $\mathbf{J}_{xc2}$ are the off-diagonal elements associated with coupling of the upper and lower mechanisms. The matrix $\mathbf{J}_x$ is a lower triangular matrix, which implies only 3 actuators

can be used for planar forces. This leads to a simple calculation [4].

From Eqn. (10), the overall Jacobian matrix **J** can be defined as

$$d\mathbf{q} = \mathbf{J}\, d\mathbf{x} \tag{13}$$

$$\text{where } \mathbf{J} = \mathbf{J}_q^{-1} \cdot \mathbf{J}_x \tag{14}$$

For force feedback, the relation between the joint torque vector $\boldsymbol{\tau}$ and the force/moment vector at the end-effector **F** needs to be found. By the principle of virtual work, the following relation holds.

$$\mathbf{F} = \mathbf{J}^T \boldsymbol{\tau} \tag{15}$$

where

$$\boldsymbol{\tau} = \{\tau_1\ \tau_2\ \tau_3\ \tau_4\ \tau_5\ \tau_6\}^T \tag{16}$$

$$\mathbf{F} = \{F_x\ F_y\ F_\theta\ F_z\ F_\phi\ F_\psi\}^T \tag{17}$$

## IV. DESIGN AND PERFORMANCE INDICES

The purpose of this section is to choose the architectural parameters based on kinematic analysis (e.g., workspace and isotropy of Jacobian). The performance indices related to the Jacobian (e.g., condition number, translationability and rotationability) is scale (unit) dependent. It is noted that the Jacobian used in this section is scaled, so that the choice of units does not influence it. The homogeneous Jacobian is defined as follows.

$$\mathbf{J}_{hxl} = \mathbf{J}_{xl} \cdot \mathrm{diag}\left[1/l_1 \quad 1/l_1 \quad 1\right] \tag{18}$$

$$\mathbf{J}_{hxu} = \mathbf{J}_{xu} \cdot \mathrm{diag}\left[1/l_1 \quad 1 \quad 1\right] \tag{19}$$

All architectural parameters employed in analysis are dimensionless parameters divided by the proximal link length, $l_1$. Despite this scaling of the Jacobian and parameters, it is still possible to depict the tendency of the kinematic characteristics with respect to the variations on the design parameters.

### A. Analysis and design of the lower mechanism.

It is desirable to achieve not only compact size but also large workspace in design of the haptic device. The radius of the design workspace should be as large as possible. But if the workspace exceeds the circle of radius, $r_l$, as seen in Fig.2, it is difficult to achieve a continuous, solid workspace that excludes any non-reachable area [7]. Further, where the limbs of the parallel mechanism are nearly folded, the Jacobian approaches zero.

Not only is it undesirable to exceed the circle of radius, $r_l$, from the kinematic viewpoint, but also the physical design of such a mechanism would be complicated and bulky. Such a design requires separate motion layers for each link (i. e., proximal link, distal link, end-effector), in order to avoid collision. Consequently, the proposed haptic master would be heavier, because of the increased complexity of the tendon structure.

For this reason, the radius of design workspace is restricted below $R_l$, and it is set to be $R_l$-r$_l$ in the analysis. The proximal link length, $l_1$ and the distal link, $l_2$, are designed to have the length of $R_l/2$ so that each limb can reach the entire workspace. The remaining parameter, $r_l$, the radius from the center of the end-effector to joints $C_i$, will be analyzed.

Even in some regions which can be reached theoretically, it is possible that the area in the bad condition is included. The dextrous workspace was suggested as the workspace that fulfils some particular dexterity conditions, *i.e.* the dexterity measure (such as the condition number of Jacobian matrix) being smaller or equal to a particular predetermined limit [8]. It is a subset of the reachable workspace.

When varying $r_l$, the reachable and dextrous workspace is shown in Fig. 6. The outer wall enveloped by lines represents the reachable workspace [9]. The dextrous workspace which is restricted by the specified condition number can be seen as meshes in the lines. The large circle on top has radius $R_l$, and the active joints are located on it. The small circle shows the designed workspace and has radius $R_l$-$r_l$.

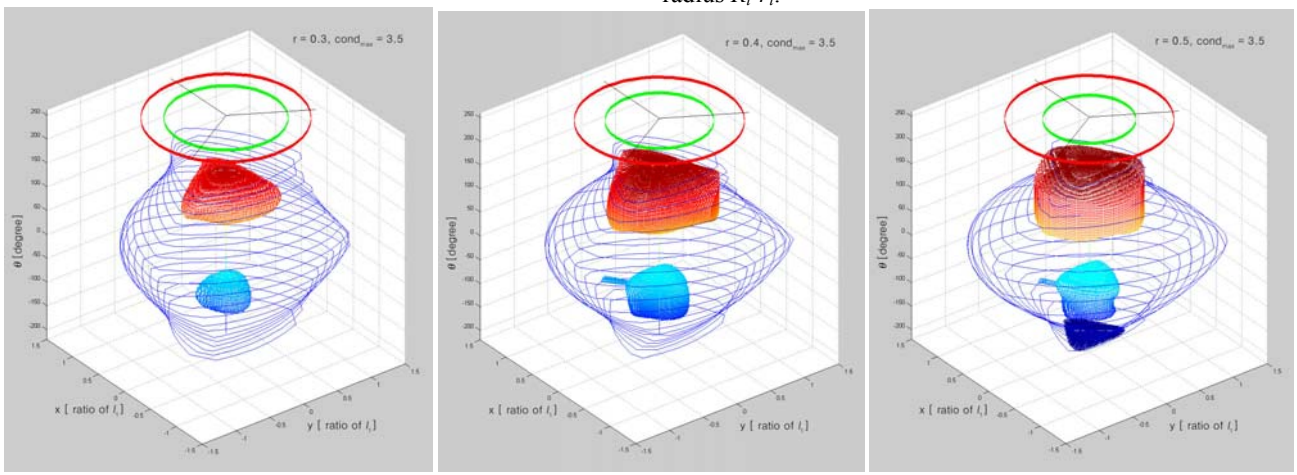


Fig. 6 Reachable and dextrous workspace of the 3RRR lower mechanism.

Other performance indices are examined for the proposed haptic master. The isotropy of the haptic master is important to apply the reflection forces evenly, and the condition number of the Jacobian is commonly used in its evaluation. The GCI (global condition index) is also examined over the whole workspace. The GCI, $\eta$, is defined as follows [10].

$$\eta = \int_W \frac{1}{c}\, dW \tag{20}$$

where $dW$ is the differential workspace volume and $c$ is the condition number of the Jacobian at a given end-effector pose.

In designing the haptic device, the capability of reflecting forces have to be estimated, and the manipulability and resistability would be useful indices for it [11]. It implies the force generated at the end-effector when the unit torque vector is loaded on the joint space. However, the reflecting torque and force on the handle would be dealt with separately in designing the haptic master. Especially in the proposed haptic master, it is important to regulate the force/torque capability between the lower and upper mechanism.

Translationability and rotationability can be used for dealing with force and torque independently [12]. For analysis, the relation between the actuator forces and the output forces, in Eqn. (15), should be rewritten.

$$\mathbf{F} = \{\mathbf{F}_f\ \mathbf{F}_\tau\}^T = \begin{bmatrix} \mathbf{J}_t^T \\ \mathbf{J}_r^T \end{bmatrix} \cdot \boldsymbol{\tau} \tag{21}$$

where $\mathbf{F}_f$ and $\mathbf{F}_\tau$ are the force and torque generated at the end-effector, and the elements in the Jacobian derived in Eqn. (14) should be rearranged into $\mathbf{J}_t$ and $\mathbf{J}_r$. Translationability and rotationability are defined as follows.

$$w_{TR} = \sqrt{\det(\mathbf{J}_t^T \cdot \mathbf{J}_t)} \tag{22}$$

$$w_{RO} = \sqrt{\det(\mathbf{J}_r^T \cdot \mathbf{J}_r)} \tag{23}$$

Because these values are configuration-dependent, the GTI (global translationability index) and GRI (global rotationability index) are used in this section as a measure for designed workspace. It is denoted as follows.

$$\zeta = \int_W w_{TR}\ dW \tag{24}$$

$$\xi = \int_W w_{RO}\ dW \tag{25}$$

The GCI, GTI and GRI are investigated for the dextrous workspace limited by the condition number, $\text{cond}_{\max} = 3.5$ and listed the table 1.

TABLE I
PERFORMANCE INDICES AT GIVEN PARAMETERS FOR LOWER MECHANISM

| $\text{cond}_{\max}$=3.5 | $r_l = 0.3$ | $r_l = 0.4$ | $r_l = 0.5$ |
|---|---|---|---|
| GCI | 0.6254 | 0.5796 | 0.5680 |
| GTI | 1.9348 | 2.0701 | 2.2167 |
| GRI | 0.5496 | 0.7131 | 0.8612 |

It is observed in Fig. 6 and Table 1, when $r_l$ increases, GTI and GRI increase, but the isotropy is on the decrease and workspace shrinks

In the actual haptic master $r_l$ is set to $0.4l_1$. The workspace of the lower mechanism is limited mechanically within the space obtained from the analysis of dextrous workspace. Not only does it ensure good configuration, but also the end-effector is initially located in the middle of the dextrous workspace.

B. Analysis and design of the upper mechanism

If the rotaion angle, $\theta$, is set to be zero in the Eqs. (6) and (7), the characteristics of the upper mechanism can be observed in isolation.

The range of $R_u$ is limited by $r_l$ because of the tendons and power transmission structure. The radius $r_u$ affects rotationability. When $r_u$ increases, it is easy to apply torque to the handle. The length of $r_u$ is chosen to be the same value as $l_3$ for simplification of the analysis, and only $l_3$ is considered a significant design parameter. The distal links no longer affect the performance when they exceed some length. It can be chosen as some reasonable value so as not to reduce stiffness.

Performance indices for given dextrous workspace and parameters are listed in Table 2. As $l_3$ increases, GRI increases, but GTI decreases. In the actual haptic master $l_3$ is set to $0.8l_1$

TABLE II
PERFORMANCE INDICES AT GIVEN PARAMETERS FOR UPPER MECHANISM.

| $\text{cond}_{\max}$=2.5 | $l_3 = 0.7$ | $l_3 = 0.8$ | $l_3 = 0.9$ |
|---|---|---|---|
| GCI | 0.4707 | 0.5227 | 0.5820 |
| GTI | 2.6340 | 2.3461 | 2.0978 |
| GRI | 1.6358 | 1.6604 | 1.6719 |

C. Analysis and design of a 6 DOF haptic master

Finally, the proposed 6 DOF mechanism is discussed based on the resulting parameters mentioned above. To achieve the balance between the lower and upper mechanism, the architectural parameters should be determined while considering GTI and GRI. It is noted that the upper and lower portions of the proposed haptic master

is coupled because of the tendon-driven mechanism. When operating the upper mechanism, a rotating torque on the lower end-effector occurs and the lower mechanism should compensate for it. Therefore, rotationability of the lower mechanism should be large enough to overcome the coupling forces. The referred performance indices are difficult to display, because the workspace has 6 dimensions. Fig. 7 represents the performance indices for the actual haptic master with respect to the variation on the position $x$ and $z$ because of the symmetry of the proposed haptic master, the result for the position $y$ is similar when the position $x$ varies. The condition number is limited below 7 over the designed workspace.

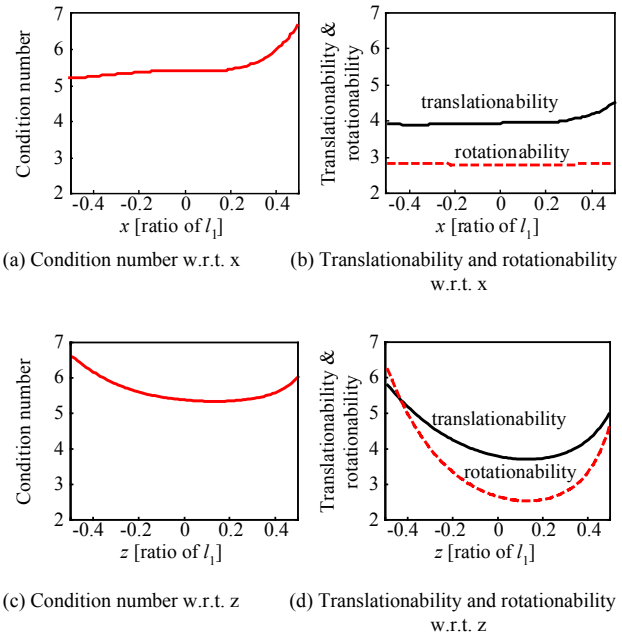


(a) Condition number w.r.t. x (b) Translationability and rotationability w.r.t. x

(c) Condition number w.r.t. z (d) Translationability and rotationability w.r.t. z

Fig. 7 Performance indices

## VI. CONCLUSION

This paper presents the kinematic analysis of a new haptic master designed to have two separate 3 DOF parallel mechanisms. Efficient actuation and reduced computational burden are achieved, since only 3 actuators are involved in planar tasks. The workspace and the performance indices related to the Jacobian are examined. The initial position of the actual system is optimized to be in the middle of the dextrous workspace. In order to balance the forces exerted between the separate mechanisms, translationability and rotationability are examined. The actual system was constructed and the architectural parameters determined based on the analysis. Further research for evaluation and improvement of the device is under way.

## VII. REFERENCES


[1] Y. Tsumaki, H. Naruse, D. N. Nenchev, and M. Uchiyama, "Design of a compact 6-DOF haptic interface," *Proc. of 1998 IEEE International Conference on Robotics and Automation*, pp. 2580-2585.

[2] G.L. Long, and C.L. Collins, "A pantograph linkage parallel platform master hand controller for force-reflection," *Proc. of 1992 IEEE International Conference on Robotics and Automation*, pp. 390-395.

[3] H. Nomo, and H. Iwata, "Presentation of multiple dimensional data by 6 DOF force display," *Proc. of 1993 IEEE/RSJ International Conference on Intelligent Robots and Systems* System, pp. 1495-1500.

[4] G. Burdea, *Force and touch feedback for virtual reality*, A Wiley-Interscience Publication, 1996.

[5] D.A. Lawrence, and J.D. Chapel, "Performance trade-offs for hand controller design," *Proc. of 1994 IEEE International Conference on Robotics and Automation*, pp. 3211-3216.

[6] D.S. Ryu, C.H. Cho, M.S. Kim and J.B.Song, "Design of a haptic master for teleoperation of a mobile manipulator," *Proc. of 2003 IEEE International Conference on Robotics and Automation*.

[7] X. J. Liu, J.S. Wang, and F. Gao, "On the optimum design of planar 3DOF parallel manipulators with respect to the workspace," *Proc. of 2000 IEEE International Conference on Robotics and Automation*, pp. 4122-27.

[8] J.A. Carretero, M. Nahon, and R.P. Podhorodeski, "Workspace analysis of a 3-dof parallel mechanism," *Proc. of 1998 IEEE/RSJ International Conference on Intelligent Robots and Systems*, pp. 1021-26.

[9] C., Gosselin, and J., Angeles, "The optimum kinematic design of a planar three degree of freedom parallel manipulator," *ASME Journal of Mechanisms, Transmissions, and Automation in Design*, Vol.110, 1988, pp. 35-41.

[10] F.Gao, X. Liu, and W.A. Gruver, "The global conditioning Index in the solution space of two degree of Freedom planar parallel manipulators," *Proc. of 1995 IEEE International Conference on Systems, Man and Cybernetics*, Vol. 5, pp. 22-25.

[11] T. Yosikawa, *Foundations of Robotics Analysis and Control*, The MIT press Cambridge.

[12] K. Kosuge, M. Okuda, T. Fukuda, T. Koduka, and T. Mizuno, "Input/output force analysis of the stewart platform type of manipulator," *Proc. of 1993 IEEE/RSJ International Conference on Intelligent Robots and Systems*, pp. 1666-1673.